Proc. Natl. Acad. Sci. USA
Vol. 80, pp. 3628–3631, June 1983
Biochemistry

Active site of RNase: Neutron diffraction study of a complex with uridine vanadate, a transition-state analog

(catalysis/enzyme structure/refinement/hydrogen bonds)

ALEXANDER WLODAWER*†, MARIA MILLER*†‡, AND LENNART SJÖLIN§

*National Measurement Laboratory, National Bureau of Standards, Washington, D.C. 20234; †Laboratory of Molecular Biology, National Institute of Arthritis, Diabetes, and Digestive and Kidney Diseases, National Institutes of Health, Bethesda, Maryland 20205; and §Department of Inorganic Chemistry, Chalmers Institute of Technology, Gothenburg, Sweden

Communicated by Isabella Karle, March 14, 1983

ABSTRACT **A complex of RNase A with a transition-state analog, uridine vanadate, has been studied by a combination of neutron and x-ray diffraction. The vanadium atom occupies the center of a distorted trigonal bipyramid, with the ribose oxygen O2′ at the apical position. Contrary to expectations based on the straightforward interpretation of the known in-line mechanism of action of RNase, nitrogen NE2 of histidine-12 was found to form a hydrogen bond to the equatorial oxygen O8, while nitrogen NZ of lysine-41 makes a clear hydrogen bond to the apical oxygen O2′. Nitrogen ND1 of histidine-119 appears to be within a hydrogen-bond distance of the other apical oxygen, O7. Two other hydrogen bonds between the vanadate and the protein are made by nitrogen NE2 of glutamine-11 and by the amide nitrogen of phenylalanine-120. The observed geometry of the complex may necessitate reinterpretation of the mechanism of action of RNase.**

Although a number of crystallographic investigations have elucidated the three-dimensional structure of RNase A (1–4) and its proteolytic modification RNase S (5–7), many details of the mechanism of action of this enzyme still remain to be conclusively determined. RNase hydrolyzes single-stranded RNA and requires a pyrimidine base on the 3′ side of the cleaved phosphodiester linkage (Fig. 1). The stereochemistry of catalysis was investigated by Usher *et al.* (8, 9), and these experiments have shown that both steps of the reaction proceed through an in-line mechanism. Although Usher did not identify the groups in the active site of the protein responsible for catalysis, these may be inferred from the published structures of RNase and of the complexes with inhibitors (6, 7, 10–12). In the first step of catalysis, histidine-12 removes a proton from the 2′ oxygen of the pyrimidine ribose, making the oxygen nucleophilic and capable of attacking the phosphorus. In the transition state, the phosphorus becomes pentacoordinated, with the 2′ and 5′ oxygens assuming apical positions. The bond between the 5′ oxygen and the ribose is cleaved, and the result of the first step of the reaction is a 2′,3′-cyclic pyrimidine nucleotide. The second step of the reaction is initiated by an attack of a water molecule activated by histidine-119 on the phosphorus opposite the 2′ oxygen, followed by formation of a pentacoordinated intermediate; finally, oxygen O2′ is protonated by histidine-12, and a 3′ nucleotide is formed. According to this interpretation, nitrogen NE2 of histidine-12 should be in the proximity of the 2′ oxygen and nitrogen ND1 of histidine-119 should be near the 5′ oxygen in order to fulfill their catalytic roles (13–15). In addition, because it has been known that lysine-41 is necessary for the catalysis and is present in the active site, this amino acid was usually placed adjacent to one of the other oxygens of the phosphate. Such a model was recently used in the design of an artificial enzyme, which showed limited RNase-like activity (16).

Lindquist *et al.* (17) postulated that a complex of uridine with oxovanadium(IV) or vanadium(V) ion could provide a stable analog of the transition state complex and they discussed a similar model. Alber *et al.* (18) studied the structure of RNase A–uridine vanadate complex by x-ray diffraction at high resolution, primarily with the aim of elucidating the importance of the flexibility of lysine-41. They have concluded that in the presence of the transition state analog, lysine-41 becomes immobilized and interacts with one of the equatorial, trigonal oxygens of the vanadate, as postulated by the theoretical studies.

Neutron diffraction is well suited for detailed investigations of the active sites of enzymes because the relatively high scattering power of atoms such as deuterium (which is routinely exchanged for hydrogen at the outset of the experiments) enables the experimenter to directly observe the protonation state of residues such as histidines and to follow the direction of hydrogen bonds (19, 20). We previously refined the structure of the native RNase by a combination of neutron and x-ray diffraction techniques at 2-Å resolution (2). The work reported here was undertaken with the aim of investigating the details of the atomic arrangement in the active site of the enzyme in the presence of the transition state analog, on the basis of results obtained in a joint neutron/x-ray refinement of a complex between RNase A and uridine vanadate.

EXPERIMENTAL PROCEDURES

By using previously described procedures (1), single crystals of RNase A were grown at pH 5.3 with 43% *t*-butyl alcohol as a precipitant. One large crystal was transferred to a vial containing 1 ml of synthetic mother liquor (without protein). Uridine vanadate solution was prepared by mixing 45 mg of uridine and 105 mg of NH_4VO_3 in 6.1 ml of imidazole buffer made in ^2H_2O (99.8% ^2H; Aldrich) and heating. The color of the resulting solution was a pale yellow. New synthetic mother liquor was prepared by mixing the uridine vanadate solution with 50% (vol/vol) deuterated methanol (Aldrich). The final pH was 6.8, and the mixture was intensely yellow. The 1 ml of solution surrounding the RNase crystal was slowly exchanged for this deuterated mother liquor, first by exchanging 10 μl 13 times, followed by 14 exchanges of 50 μl each. The solution volume was then reduced to 0.5 ml, and 100 μl was exchanged 20 times. The whole exchange process took 3 months, and the final solution contained <1% of the original amount of hydrogen. Upon completion of the exchange, a number of small pieces were cut from the crystal with a scalpel blade, and a large piece (4.5 × 3.5 × 1.2 mm) was mounted in a quartz tube as described (21). Neutron data were measured with the flat-cone diffractometer

The publication costs of this article were defrayed in part by page charge payment. This article must therefore be hereby marked "*advertisement*" in accordance with 18 U.S.C. §1734 solely to indicate this fact.

‡Current address: Dept. of Chemistry, The University of Texas, Austin, TX 78712.

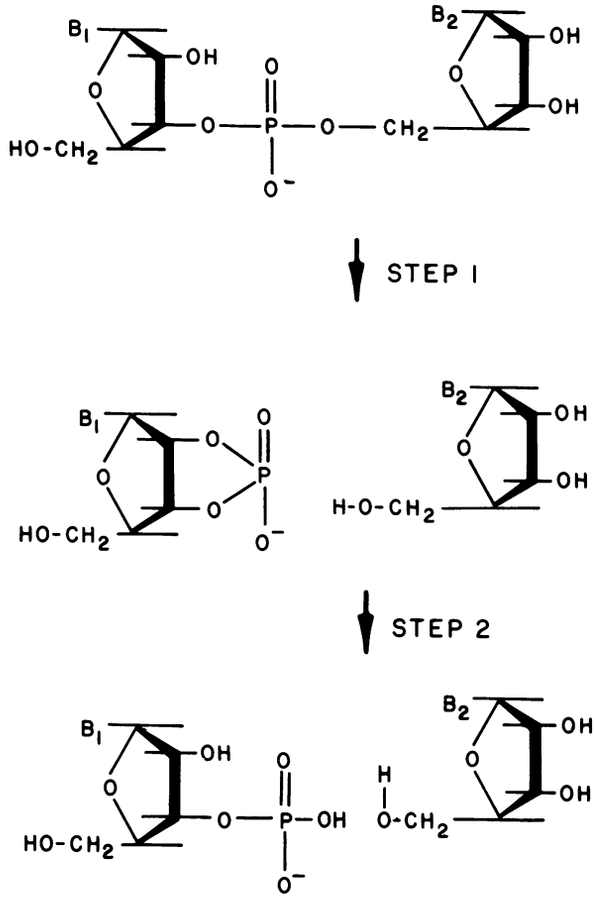

FIG. 1. The chemical reaction catalyzed by pancreatic RNase. Site B_1 is always occupied by a pyrimidine, whereas either pyrimidine or purine may occupy the site B_2.

installed at the National Bureau of Standards reactor (22). Unit cell parameters of the crystal changed slightly after soaking and became $a = 30.3$ Å, $b = 30.35$ Å, $c = 53.7$ Å, $\beta = 106.4°$. Because of the difficulty encountered in orienting the crystal in the tube, the crystallographic c axis was set parallel to the tube axis (and thus to the axis of rotation). This slowed the data collection by 35% compared to the optimum mounting around the a axis but caused no other difficulties. Reflection intensities were integrated by using a "dynamic mask procedure" (23). Absorption correction was applied by using a published procedure (24). The absorption curve was synthesized by comparing the intensities of equivalent reflections found in different ranges of the rotation angle ψ (25). Such a curve was found to be superior to the usual one obtained by rotating an axial reflection around its diffraction vector because the tube was inclined by about 45° to the rotation axis. Reflections that could not be recorded with the flat-cone method and levels with h between 0 and 3 were measured by using equatorial geometry. These data were later used for scaling. The symmetry R factor ($R_{sym} = \Sigma |F_i - \bar{F}|/\Sigma n \bar{F}$) varied between 0.039 and 0.060 for different levels, and the scaling R for the equatorial and flat-cone data was 0.063. After final scaling, the number of unique observed data [$I > 1.5\sigma(I)$] was 6,315, which corresponded to 73% of all possible data to 2-Å resolution, with an extra 8% of possible reflections in the shell of 2–1.75 Å. Although these high-resolution reflections were retained in the refinement, we considered the nominal resolution of the data to be only 2 Å.

X-ray data were measured from a single fragment of the original crystal, thus assuring identical deuteration and substitution of the inhibitor. The crystal was mounted in a glass capillary and was jammed in cotton fibers (26), primarily to prevent its motion. Reflections were collected by using a limited ω step scan and were integrated by using an algorithm of Hanson *et al.* (27). The number of significant reflections in the 2- to 10-Å resolution range was 6,617, 85% of those theoretically accessible.

The refinement of the structure of the complex was accomplished by using an algorithm of Wlodawer and Hendrickson (28) in which the model is refined with both neutron and x-ray data. The structure of the native RNase refined with the x-ray and neutron data (2) provided a point of departure. A standard group for uridine vanadate was prepared by modifying a model provided by W. Gilbert and G. A. Petsko. The inhibitor could be fitted easily to x-ray and neutron difference Fourier maps calculated with the phases based on the native model. No restraints were placed on the bond angles of the oxygens surrounding the vanadium atom, whereas the usual restraints were placed on the remaining parts of the inhibitor and on the protein. After each six or seven cycles of refinement, the model was examined and adjusted by using computer graphics (29), and the procedure was repeated through a total of four refinement and rebuilding cycles.

The final model resulting from the joint refinement was characterized by standard crystallographic R factors of 0.191 (x-ray) and 0.207 (neutron), with root-mean-square deviations of bond length from ideality of 0.024 Å (bonds not involving hydrogen) and 0.021 Å (bonds involving hydrogen). The root-mean-square shift of the nonhydrogen protein coordinates from the initial model was 0.38 Å.

RESULTS AND DISCUSSION

Although both the x-ray and neutron difference Fourier maps were reasonably clear even before the commencement of the refinement procedures, they were improved further after the refinement. The only area of the map of the inhibitor that was not clear was in the vicinity of the 3′ carbon of the sugar, and this may have been a reason for some difficulty encountered in establishing the sugar pucker. The areas corresponding to the base of uridine were markedly asymmetric, leaving no doubt about the *anti* conformation of the glycosidic bond. The good quality of the neutron map was attested by the fact that even though the deuterium attached to the 5′ oxygen of the ribose was never placed in the model of the inhibitor, the density at its position was nevertheless clearly visible in the final map. The x-ray and neutron densities were also clear for all the amino acid side chains involved in the catalytic activity. Both histidines appeared to be protonated, in agreement with the increase of the pK of these groups in the presence of inhibitors observed by NMR (30). The movement of these side chains did not exceed 0.2 Å from the positions observed in the native structure of RNase. The end group of lysine-41 moved 0.6 Å from the position found in the native enzyme, and the average temperature factor for this side chain was lowered from 20 to 8 Å^2, in agreement with the results of Alber *et al.* (18). No major movement of other groups was detected in the area of the active site.

The three-dimensional arrangement of the inhibitor and of the surrounding side chains of the protein is shown in Fig. 2. As expected on the basis of theoretical considerations (17), the vanadium atom lies in the center of a distorted trigonal bipyramid with the oxygens O2′ and O7 found in the apical positions, while the oxygens O3′, O6, and O8 lie in the basal plane. The distance of the vanadium atom V from the best least-squares plane formed by V, O3′, O6, and O8 is 0.085 Å. The angle formed by O2′-V-O7 is 156°, indicating the distortion in the bipyramid.

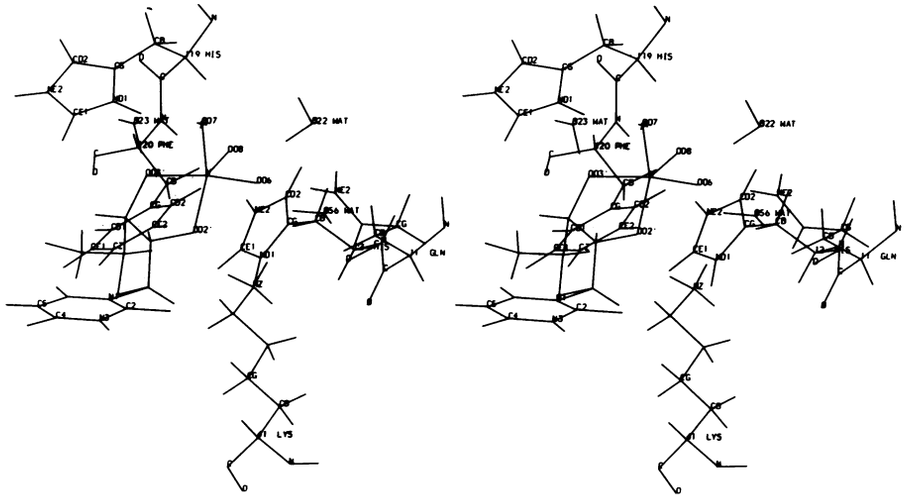

FIG. 2. Interaction of uridine vanadate with selected residues that form the active site of RNase (Gln-11, His-12, Lys-41, His-119, and Phe-120). See text for details.

This angle was refined to within 5° independently of the type of restraints placed on the standard group.

Unexpectedly, the hydrogen bonds formed between the side chains of RNase and the oxygens surrounding the vanadium atom did not appear to conform to the predictions based on the theoretical considerations (13–15). In particular, it is lysine-41 rather than histidine-12 that appears to be hydrogen bonded to the apical O2′ oxygen (Fig. 3). The distance between the nitrogen NZ of lysine-41 and oxygen O2′ is 2.79 Å, and the angle NZ-^{2}HZ1-O2′ is 165°. There is a clear indication of a continuous density in the neutron difference Fourier map, as expected at this resolution for hydrogen-bonded atoms. The distance between nitrogen NZ of lysine-41 and the closest equatorial oxygen of the bipyramid (O6) is 3.38 Å, with no indication of a hydrogen bond. Conversely, nitrogen NE2 of histidine-12 is 2.62 Å from the equatorial oxygen O8, with the angle NE2-^{2}HE2-O8 of 160°. Again, these atoms are connected by a continuous density in the neutron Fourier map. The distance between nitrogen NE2 of histidine-12 and oxygen O2′ is 3.22 Å, with no indication of a hydrogen bond.

According to the theoretical model discussed above, histidine-119 was expected to be in the vicinity of the other apical oxygen of the bipyramid. The distance between the nitrogen ND1 of histidine-119 and the equatorial oxygen O3′ is 2.66 Å, while its distance from the apical oxygen O7 is 3.03 Å. Nevertheless, the neutron density indicates that the latter hydrogen bond is more probable. There is little indication that the oxygen O7 is protonated. In the hypothetical model of the complex (17), this position was occupied by a coordinated water molecule. The bond length between oxygen O7 and vanadium is 1.99 Å. A water molecule is located in a well-defined peak close to the oxygens O7 and O3′.

Other clear hydrogen bonds between the amino acid side chains and the vanadate include a 3.12-Å-long bond between

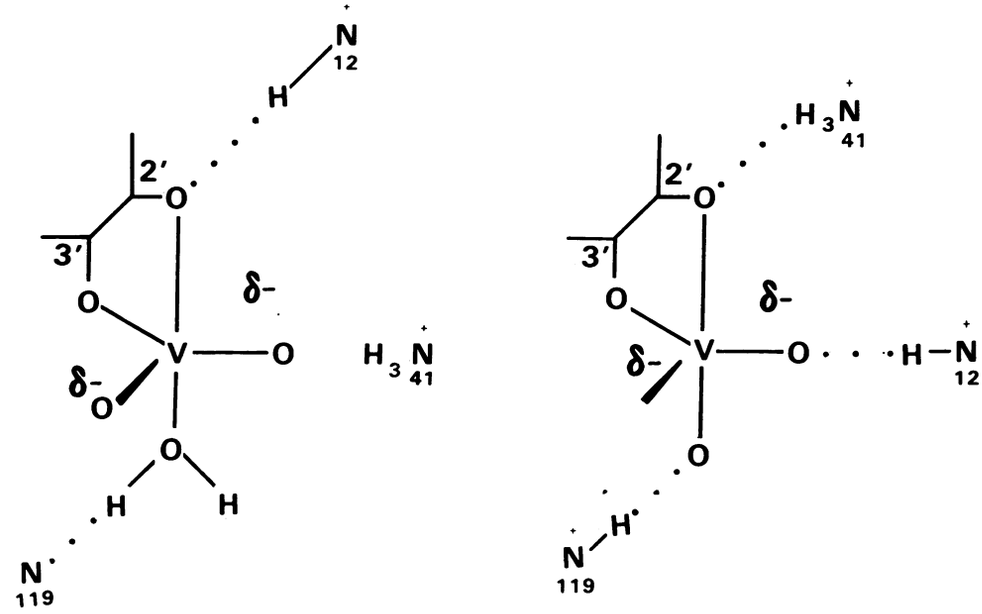

FIG. 3. (*Left*) Hypothetical partial structure for the complex of RNase with uridine vanadate, postulated by Lindquist *et al.* (17). (*Right*) Diagram of the structure observed in the current investigation. It should be noted that although both histidines are observed to be protonated, it is likely that the presence of some unprotonated residues is necessary for the catalytic activity.

the nitrogen of phenylalanine-120 and oxygen O8 and a 2.48-Å-long bond between nitrogen NE2 of glutamine-11 and oxygen O6. Another water molecule can be found 2.69 Å from oxygen O8. Contrary to some predictions (15), lysine-7 does not make direct contacts with the nucleoside.

Several separate refinements, each using either a modified standard group for uridine vanadate or different restraints, did not change the atomic arrangement described above in any significant way. Although the lengths of the individual hydrogen bonds varied by up to 0.1 Å, no alternative bonding ever emerged, and further refinement of the current model is not expected to change it in an appreciable way.

The interpretation of the results presented here and their reconciliation with the mechanistic model is not straightforward. The in-line model of the catalytic action (8, 9) is well established, and the observed atomic arrangement of the bipyramid is in good agreement with the requirement that the leaving groups in both the first or the second step of the reaction should always be apical. It is improbable that a group other than histidine could act as both a general acid and a general base during the catalysis; thus, the observed hydrogen-bonding pattern may indicate that the proton transfers do not follow the simplest route. It is unlikely that the amino group of lysine-41 could assume the role of general acid–general base, even though it forms a clear hydrogen bond with the apical oxygen of the complex. It is also unclear why the temperature factor of lysine-41 is lowered by a factor of 2.5 compared to that in the native structure, where a hydrogen bond to the phosphate is also made (2).

Although a number of stuctures of the RNase S complexes with mono- and dinucleotides have been studied by x-ray diffraction, none of them has been subjected to least-squares refinement; thus, the published details of the interaction between the substrate and the protein should be regarded with caution. Whereas Pavlovsky *et al.* (12) interpreted the structure of 2′-fluorouridylyl(3′-5′)cytidine to indicate that the fluorine (occupying the site of the 2′-oxygen of the normal substrate) was within a potential hydrogen bond distance to histidine-12, their conclusions may not be wholly justified by the quality of their difference Fourier map. This interpretation was also contradicted by Wodak *et al.* (11), who found that in the complex of RNase S with cytidylyl(2′,5′)-adenosine, the oxygen closest to the nitrogen NE2 of histidine-12 was O(II), while oxygen O2′ was farther away. The distortion introduced by the presence of the 2′,5′ linkage rather than of the usual 3′,5′ linkage and the limited refinement of the model make it necessary to treat the results of Wodak *et al.* with some caution. These two studies left the question of the position of lysine-41 open because neither group could see the density corresponding to that residue in the respective Fourier maps. The orientation of histidine-119 was also less clear than that of histidine-12.

Some support for our results comes from previous NMR studies. Jentoft *et al.* (31) investigated the resonances in the [^{13}C]-methylated RNase A and concluded that lysine-41 must interact with a histidine, which was identified by them as histidine-12. They also found evidence for the interaction of lysine-41 with the 2′ oxygen of the ribose and suggested that lysine-41 might aid in the deprotonation of the 2′ hydroxyl group prior to forming the 2′,3′-cyclic intermediate. These NMR results are in excellent agreement with the structure observed by us.

However, it should be stressed that the structure presented here does not offer direct proof that uridine vanadate is indeed a proper transition state analog, and some caution in the interpretation of our results is necessary. An unambiguous picture of the active site in different stages of catalysis may emerge after high-resolution structures of the complexes with the substrate and with the product become available (18). Nevertheless, the results presented here should enhance our knowledge of the three-dimensional structure of the active site of RNase and should attest to the usefulness of neutron diffraction and least-squares refinement in such studies.

We thank Drs. David Davies and Paulina Wlodawer for critical reading of the manuscript.

1. Wlodawer, A., Bott, R. & Sjölin, L. (1982) *J. Biol. Chem.* **257**, 1325–1332.
2. Wlodawer, A. & Sjölin, L. (1983) *Biochemistry*, in press.
3. Borkakoti, N., Moss, D. A. & Palmer, R. A. (1982) *Acta Crystallogr. Sect. B* **38**, 2210–2217.
4. Borkakoti, N., Moss, D. A., Stanford, M. J. & Palmer, R. A. (1983) *J. Mol. Biol.*, in press.
5. Wyckoff, H. W., Tsernoglou, D., Hanson, A. W., Knox, J. R., Lee, B. & Richards, F. M. (1970) *J. Biol. Chem.* **245**, 305–328.
6. Richards, F. M. & Wyckoff, H. W. (1971) in *The Enzymes*, ed. Boyer, P. D. (Academic, New York), 3rd Ed., Vol. 4, pp. 647–806.
7. Richards, F. M. & Wyckoff, H. W. (1973) *Atlas of Molecular Structures in Biology, 1. Ribonuclease S*, eds. Phillips, D. C. & Richards, F. M. (Clarendon, Oxford).
8. Usher, D. A., Richardson, D. I. & Eckstein, F. (1970) *Nature (London)* **228**, 663–665.
9. Usher, D. A., Erenrich, E. S. & Eckstein, F. (1972) *Proc. Natl. Acad. Sci. USA* **69**, 115–118.
10. Wyckoff, H. W., Carlson, W. & Wodak, S. (1977) in *Nucleic Acid-Protein Recognition*, ed. Vogel, H. J. (Academic, New York), pp. 569–580.
11. Wodak, S. Y., Liu, M. Y. & Wyckoff, H. W. (1977) *J. Mol. Biol.* **116**, 855–875.
12. Pavlovsky, A. G., Borisova, S. N., Borisov, V. V., Antonov, I. V. & Karpeisky, M. Ya. (1978) *FEBS Lett.* **92**, 258–262.
13. Holmes, R. R., Deiters, J. A. & Gallucci, J. C. (1978) *J. Am. Chem. Soc.* **100**, 7393–7402.
14. Deakyne, C. A. & Allen, L. C. (1979) *J. Am. Chem. Soc.* **101**, 3951–3959.
15. Umeyama, H., Nakagawa, S. & Fuji, T. (1979) *Chem. Pharm. Bull.* **27**, 974–980.
16. Breslow, R. (1982) *Science* **218**, 532–537.
17. Lindquist, R. N., Lynn, J. L. & Lienhard, G. E. (1973) *J. Am. Chem. Soc.* **95**, 8762–8768.
18. Alber, T., Gilbert, W. A., Ponzi, D. R. & Petsko, G. A. (1983) *Ciba Symp.* **93**, 4–24.
19. Wlodawer, A. & Sjölin, L. (1981) *Proc. Natl. Acad. Sci. USA* **78**, 2853–2855.
20. Wlodawer, A. (1982) *Prog. Biophys. Mol. Biol.* **40**, 115–159.
21. Wlodawer, A. (1980) *Acta Crystallogr. Sect. B* **36**, 1826–1831.
22. Prince, E., Wlodawer, A. & Santoro, A. (1978) *J. Appl. Crystallogr.* **11**, 173–178.
23. Sjölin, L. & Wlodawer, A. (1981) *Acta Crystallogr. Sect. A* **37**, 594–604.
24. Santoro, A. & Wlodawer, A. (1980) *Acta Crystallogr. Sect. A* **36**, 442–450.
25. Xuong, N. H., Freer, S. T., Hamlin, R., Nielsen, C. & Vernon, W. (1978) *Acta Crystallogr. Sect. A* **34**, 289–296.
26. Narayana, S. V. L., Weininger, M. S., Heuss, K. L. & Argos, P. (1982) *J. Appl. Crystallogr.* **15**, 571–573.
27. Hanson, J. C., Watenpaugh, K. D., Sieker, L. & Jensen, L. H. (1979) *Acta Crystallogr. Sect. A* **35**, 616–621.
28. Wlodawer, A. & Hendrickson, W. H. (1982) *Acta Crystallogr. Sect. A* **38**, 239–247.
29. Jones, T. A. (1978) *J. Appl. Crystallogr.* **11**, 268–272.
30. Cohen, J. S., Hughes, L. J. & Wooten, J. B. (1983) in *Magnetic Resonance in Biology*, ed. Cohen, J. S. (Wiley, New York), Vol. 2, pp. 130–247.
31. Jentoft, J. E., Gerken, T. A., Jentoft, N. & Dearborn, D. G. (1981) *J. Biol. Chem.* **256**, 231–236.